Cell Stem Cell
Article

Cdc42 Activity Regulates Hematopoietic Stem Cell Aging and Rejuvenation

Maria Carolina Florian,[1] Karin Dörr,[1] Anja Niebel,[1] Deidre Daria,[1] Hubert Schrezenmeier,[2] Markus Rojewski,[2] Marie-Dominique Filippi,[3] Anja Hasenberg,[4] Matthias Gunzer,[4] Karin Scharffetter-Kochanek,[1] Yi Zheng,[3] and Hartmut Geiger[1,3,*]

[1]Department of Dermatology and Allergic Diseases
[2]Institute for Clinical Transfusion Medicine and Immunogenetics Ulm
University of Ulm, 89091 Ulm, Germany
[3]Division of Experimental Hematology and Cancer Biology, Cincinnati Children's Hospital Medical Center and University of Cincinnati, Cincinnati, OH 45229-3026, USA
[4]Institute of Experimental Immunology and Imaging, University Hospital, Universität Duisburg/Essen, 45141 Essen, Germany
*Correspondence: hartmut.geiger@uni-ulm.de
DOI 10.1016/j.stem.2012.04.007

SUMMARY

The decline in hematopoietic function seen during aging involves a progressive reduction in the immune response and an increased incidence of myeloid malignancy, and has been linked to aging of hematopoietic stem cells (HSCs). The molecular mechanisms underlying HSC aging remain unclear. Here we demonstrate that elevated activity of the small RhoGTPase Cdc42 in aged HSCs is causally linked to HSC aging and correlates with a loss of polarity in aged HSCs. Pharmacological inhibition of Cdc42 activity functionally rejuvenates aged HSCs, increases the percentage of polarized cells in an aged HSC population, and restores the level and spatial distribution of histone H4 lysine 16 acetylation to a status similar to that seen in young HSCs. Our data therefore suggest a mechanistic role for Cdc42 activity in HSC biology and epigenetic regulation, and identify Cdc42 activity as a pharmacological target for ameliorating stem cell aging.

INTRODUCTION

In the hematopoietic system, aging is driven by both intrinsic and extrinsic factors (Chambers and Goodell, 2007; Dorshkind and Swain, 2009; Geiger et al., 2005; Geiger and Van Zant, 2002; Ju et al., 2007; Morrison et al., 1996; Rando, 2006; Rossi et al., 2005) and manifests as decreased immune response (Linton and Dorshkind, 2004), increased myelogenous disease (Kiss et al., 2007; Signer et al., 2007), late-onset anemia (Beghé et al., 2004), and reduced regenerative capacity (Ergen and Goodell, 2009). Multiple studies and our own data demonstrate that the aged murine hematopoietic system is impaired in supporting peripheral blood (PB) leukocyte numbers (Figure S1A available online), erythropoiesis (Figures S1B and S1C), and B-lymphoid and T-lymphoid cells (Figure S1D), while the number of myeloid cells is increased (Figure S1D). Changes in the total number of primitive hematopoietic cells with age are strain dependent (Kamminga et al., 2005) and are at least in part intrinsic to hematopoietic stem cells (HSCs). For example, in C57BL/6 mice, early hematopoietic progenitor cell (Lineage^{neg}c-Kit^{+}Sca-1^{+}, or LSK) and long-term repopulating-HSC (LSKCD34$^{low/-}$Flk2^{-}, LT-HSCs) numbers increase with age (Figures S1E and S1F), while numbers of lymphoid-primed multipotent progenitors (LMPPs, LSKCD34^{+}Flk2^{+}; Adolfsson et al., 2005) decrease (Figure S1F). Independent of the strain, aged HSCs show reduced self-renewal activity as determined in serial transplant/engraftment assays (Janzen et al., 2006; Rossi et al., 2005) and exhibit a 2-fold reduced ability to home to the bone marrow (BM) (Liang et al., 2005). Moreover, aged LSKs are less efficient in their ability to adhere to stroma cells and exhibit significantly elevated cell protrusion activity in vivo (Geiger et al., 2007; Kohler et al., 2009; Xing et al., 2006). Thus, a defined set of cell-intrinsic phenotypic and functional parameters separate young from aged HSCs. Due to the cell-intrinsic component of HSC aging—aged HSCs present with most of these phenotypes also when exposed to a young microenvironment—one refers to young HSCs and aged HSCs when speaking of HSCs from young and aged animals (Geiger and Rudolph, 2009).

Cdc42 belongs to the family of small RhoGTPases and cycles between an active (GTP-bound) and an inactive (GDP-bound) state. Cdc42 is known to regulate actin and tubulin organization, cell-cell and cell-extracellular matrix adhesion, and cell polarity in distinct cell types (Cau and Hall, 2005; Etienne-Manneville, 2004; Florian and Geiger, 2010; Sinha and Yang, 2008). Our previous and current studies demonstrate that Cdc42 activity is significantly increased in both primitive hematopoietic cells (Figure S1G) and other tissues of aged mice when compared with that in cells from young animals (Xing et al., 2006). Based on this observation we hypothesize that the aging-associated increased Cdc42 activity in HSCs may causatively regulate cell-intrinsic aging of HSCs (Geiger et al., 2007; Kohler et al., 2009).

RESULTS

Constitutively Increased Cdc42 Activity Results in Aging-like Phenotypes in Young HSCs

To test the role of Cdc42 activity in cell-intrinsic aging of HSCs, we determined whether Cdc42 activity in young HSCs

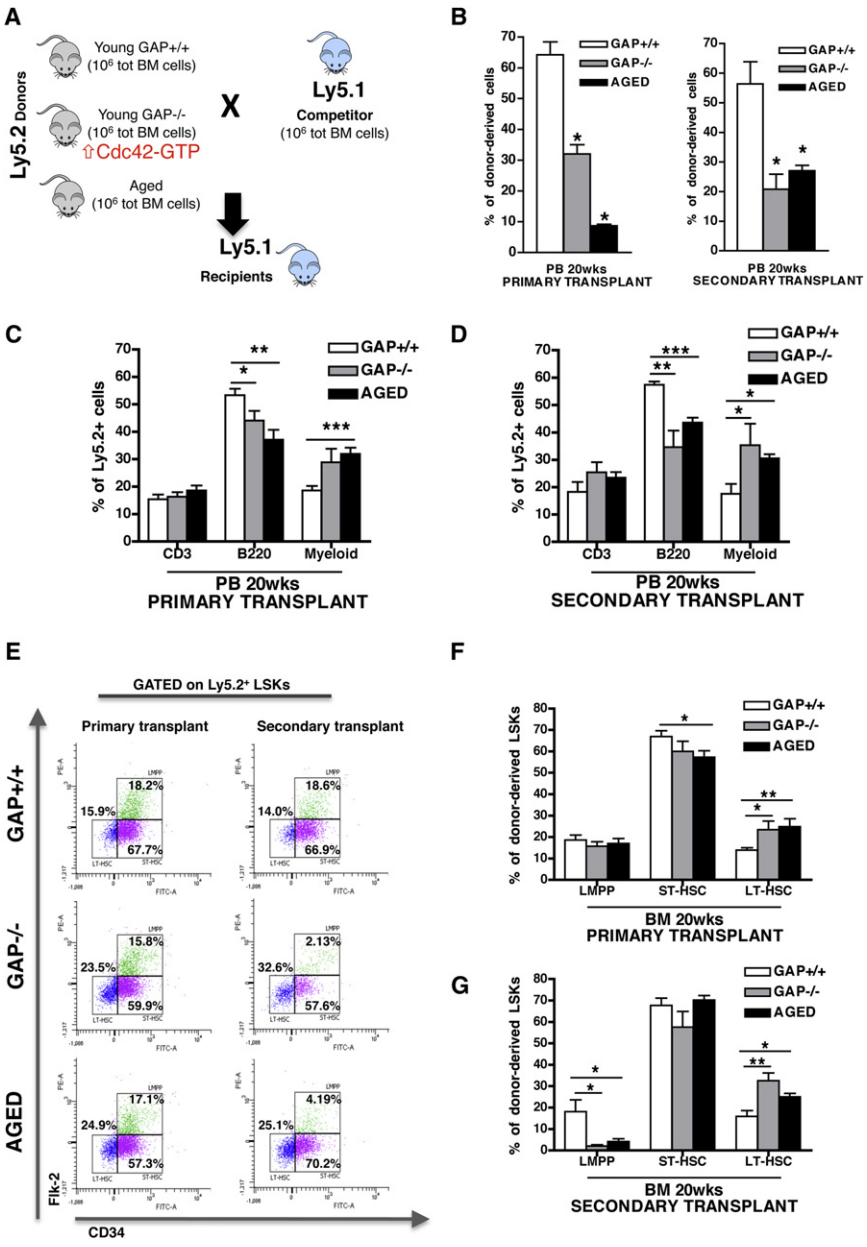

Figure 1. Constitutively Increased Cdc42 Activity Results in Premature Aging of Young HSCs

(A) Scheme of the experimental set-up for the competitive BM transplants.

(B) Contribution of total donor-derived Ly5.2$^+$ cells in PB after 20 weeks in competitive primary and secondary transplants. Percentages of engrafted cells are normalized according to stem cell equivalent. Mice were considered as engrafted when the percentage of Ly5.2$^+$ cells in PB was higher than 1.0 and contribution was detected for all PB lineages.

(C and D) Contribution of B cells, T cells, and myeloid cells among donor-derived Ly5.2$^+$ cells in PB after 20 weeks in competitive primary (C) and secondary (D) transplants.

(E–G) Representative FACS dot plots (E) and quantitative and statistical analysis of LT-HSC, ST-HSC, and LMPP distribution among donor-derived LSKs in primary (F) and secondary (G) transplanted mice. *p < 0.05, **p < 0.01, ***p < 0.001; columns are means +1 SE. The experiment was repeated three times with a cohort of four or five recipient mice per group (n = 14).

See also Figure S1.

constitutively increased by genetic means is sufficient to resemble aging-like phenotypes in HSCs, using as a model HSCs deficient for the p50RhoGAP protein (*Cdc42GAP*$^{-/-}$ mice). This RhoGAP protein is a highly selective negative regulator of Cdc42 activity (Barfod et al., 1993), and therefore *Cdc42GAP*$^{-/-}$ mice present with a gain of activity specific for Cdc42 in all tissues (Wang et al., 2007), including primitive hematopoietic cells (Figures S1I). Supporting our hypothesis, *Cdc42GAP*$^{-/-}$ mice present with premature aging-like phenotypes in multiple tissues and cell types (Wang et al., 2007). As for the hematopoietic system, a significant increase in myeloid cell frequency and a decrease in T cell frequency in PB was detected in young *Cdc42GAP*$^{-/-}$ mice as well as an overall decrease of B cell frequency and an increase in myeloid cell frequency in BM, which are phenotypes consistent with aging in hematopoiesis (Figure S1J). To determine the functional status of *Cdc42GAP*$^{-/-}$ HSCs, competitive serial transplant assays were performed (Figure 1A), which are regarded as a gold standard for determining stem-cell-intrinsic parameters of HSC aging (Chambers and Goodell, 2007; Rossi et al., 2005, 2008). Results demonstrated that young *Cdc42GAP*$^{-/-}$ HSCs resemble aged HSCs and were significantly distinct from young control *Cdc42GAP*$^{+/+}$ HSCs with respect to their repopulation ability (Figure 1B), contribution to the B cell lineage, and contribution to the myeloid cell lineage in PB (Figures 1C and 1D) and BM (Figures S1M and S1N) in both primary and secondary recipients. Furthermore, young *Cdc42GAP*$^{-/-}$ cells, similarly to aged cells, contributed significantly more to the pool of LT-HSCs compared with young *Cdc42GAP*$^{+/+}$ controls both in primary and in secondary recipients (Figures 1E–1G). There was also a significant decrease in the contribution of aged and *Cdc42GAP*$^{-/-}$ HSCs to LMPPs in secondary recipients compared with that of young *Cdc42GAP*$^{+/+}$ cells (Figure 1G). Thus, chronologically young *Cdc42GAP*$^{-/-}$ HSCs are functionally similar to chronologically aged HSCs in competitive transplantation assays. These data imply a mechanistic role for intrinsically elevated Cdc42 activity in chronologically aged HSCs for phenotypic and functional changes associated with aged HSCs.

Increased Cdc42 Activity in HSCs Correlates with a Depolarized Phenotype in LT-HSCs

In *D. melanogaster*, the age-associated loss of germline stem cell function correlates with loss of cell polarity (Cheng et al.,

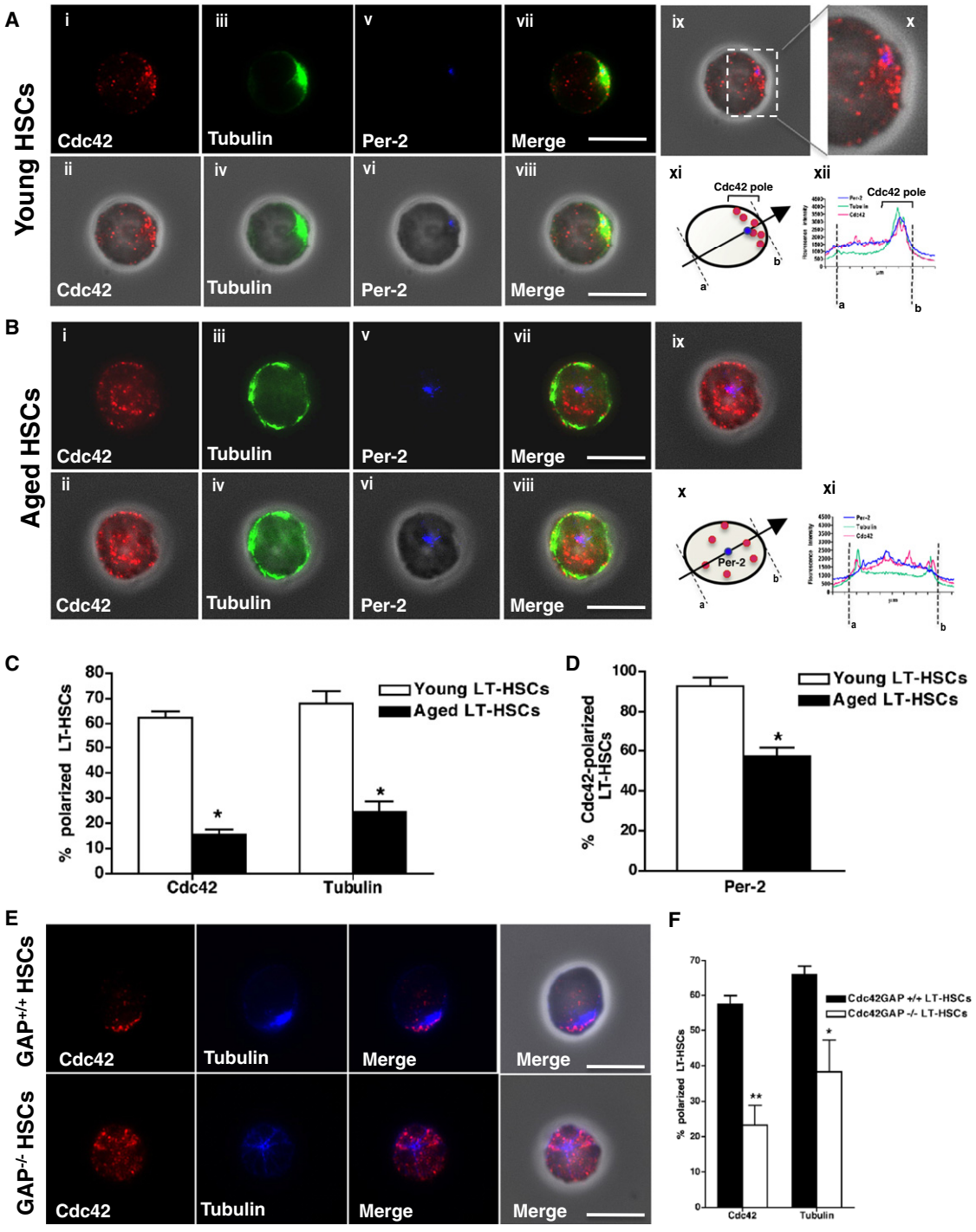

Figure 2. Increased Cdc42 Activity Correlates with a Depolarized Phenotype in LT-HSCs

(A) Representative distribution of Cdc42, tubulin, and pericentrin-2 (Per-2) in young LT-HSCs determined by IF. Pictures are shown on a dark background (panels i, iii, v, and vii) or as overlap with the phase contrast picture (panels ii, iv, vi, and viii). Bar = 5 μm. Panels ix and x show Cdc42 (red) and Per-2 (blue) distribution over the phase contrast picture. Panel xi: schematic presentation of a representative distribution of Cdc42 in young LT-HSCs (Per-2, blue dot; Cdc42, red dots). The arrow indicates the direction from "a" to "b" followed for determining fluorescence intensity in panel xii. Panel xii: representative fluorescence intensity plot obtained by collecting pixel intensity through the section of the cell as indicated in panel xi.

(B) Representative distribution of Cdc42, tubulin, and Per-2 in aged LT-HSCs determined by IF. Pictures are shown on a dark background (panels i, iii, v, and vii) or as overlap with the phase contrast picture (panels ii, iv, vi, and viii). Bar = 5 μm. Panel ix shows Cdc42 (red) and Per-2 (blue) distribution over the phase contrast picture. Panel x: schematic presentation of a representative distribution of Cdc42 in aged LT-HSCs (Per-2, blue dot; Cdc42, red dots). The arrow indicates the direction from "a" to "b" followed for determining fluorescence intensity in panel xi. Panel xii: representative fluorescence intensity plot obtained by collecting pixel intensity through the section of the cell as indicated in panel x.

2008). We recently reported a reduction in the frequency of cells with a polar distribution of microtubules among aged early hematopoietic progenitor cells (LSK cells) (Kohler et al., 2009). Cdc42 activity has been implicated in the regulation of polarity in fibroblasts and epithelial cells (Cau and Hall, 2005; Iden and Collard, 2008) and in the maintenance of polarity and stemness in neuronal stem cells (Cappello et al., 2006). Prompted by these observations we next investigated whether the polarity status of LT-HSCs changes upon aging, and whether Cdc42 activity might be causally involved in regulating such changes. To test this we initially determined the localization of Cdc42, which in itself is a cell polarity marker (Etienne-Manneville, 2004), and tubulin in LT-HSCs in single-cell immunofluorescence (IF) analyses performed on LT-HSCs. Interestingly, in the majority of young LT-HSCs, Cdc42 and tubulin were asymmetrically distributed and were found at the same location inside the cell (Figures 2A and 2C, Figures S2A and S2C, and Movie S1). This highly asymmetric localization of Cdc42 and tubulin did not correlate with the side of the cell bound to the substrate or with an uneven distribution of the whole cytoplasm, because, for example, F-actin always showed a cortical and unpolarized distribution (Figures S2E and S2F and Movie S2). The asymmetry was oriented along the xy plane on one side of the nucleus, where the centrosome was also localized (Figure 2A panels ix–xii and Movie S1). Therefore, in young LT-HSCs, Cdc42 and the microtubules were highly concentrated in the immediate pericentriolar zone and in the cytoplasmatic space along the nucleus/centrosome/cell membrane axis (Figures 2A and 2D, Movie S1). In contrast, Cdc42 and tubulin were distributed throughout the cell body in an unpolarized fashion in aged LT-HSCs (Figures 2B and 2C, Figures S2B, S2D, and S2F, and Movie S3), and the centrosome was mostly found in the middle of the cell, oriented perpendicularly to the nucleus along the z axis (Figure 2B panels ix–xi, Figure 2D, and Movie S3). Similar results (young HSCs polar, aged HSCs apolar) were also obtained by analyzing additional established cell polarity markers like Crumbs3 (Figures S2G, S2I, and S2J) and Dgl (Figures S2G and S2K). Par6 (Figures S2G and S2L) and the aPKCζ (Figure S2G) did not follow this pattern, in agreement with recently published data (Sengupta et al., 2011). Interestingly, the difference in polarity among young and aged primitive hematopoietic cells is specific to LT-HSCs because, for example, we did not observed a difference between young and aged short-term (ST)-HSCs (Figure S2H), and it is not correlated to the cycle status, because young and aged LT-HSCs show very similar cell cycle parameter profiles (Figure S1H and also Chambers et al., 2007; Rossi et al., 2007; Silva and Conboy, 2008; Sudo et al., 2000). In summary, chronologically young HSCs present with a polarity phenotype similar to the one previously described for memory T cells (Chang et al., 2007; Ludford-Menting et al., 2005)—which is lost upon aging of LT-HSCs. Recently CD150 expression was described as a marker for functionally distinct subpopulations within the pool of LT-HSCs (Beerman et al., 2010). The polarity phenotype identifying phenotypically different types of LT-HSCs (polar versus apolar) might thus constitute another surrogate marker for the distinct cell subsets stained by CD150 expression. The frequency of young LT-HSCs polarized for Cdc42 and tubulin though was independent of the expression of CD150 on LT-HSCs (Figures S2M and S2N).

Consistent with a critical role of elevated Cdc42 activity in age-associated phenotypes like apolarity, IF staining revealed that the majority of chronologically young *Cdc42GAP*$^{-/-}$ LT-HSCs, which functionally resemble aged LT-HSCs, were apolar with respect to Cdc42 and tubulin distribution (Figures 2E and 2F). In addition, consistent with our observations comparing chronologically young and aged LT-HSCs (Figure S1H), young *Cdc42GAP*$^{+/+}$, *Cdc42GAP*$^{-/-}$ and aged LT-HSCs present with a similar cell cycle and apoptosis profile (Figures S1K and S1L), strongly implying that differences in polarity are independent of these parameters. These data thus identify Cdc42 as a polarity protein in LT-HSCs showing distinct polarity phenotypes in young and aged LT-HSCs, and support at a role for Cdc42 activity specifically in the regulation of LT-HSC polarity.

Pharmacological Reduction of Cdc42 Activity Rejuvenates Aged LT-HSC Function and Restores the Level and the Spatial Distribution of Histone H4 Lysine 16 Acetylation

Our data imply that the aging-associated increase in Cdc42 activity might be a stem-cell-intrinsic molecular mechanism resulting in both apolarity and impaired function of LT-HSCs with age. We consequently reasoned that inhibiting Cdc42 activity in aged LT-HSCs to the level in young LT-HSCs by pharmacological means might be a possible approach to at least in part revert apolarity as well as the impaired function of aged LT-HSCs. To exclude stem-cell-extrinsic effects and focus on cell-intrinsic mechanisms, LT-HSCs from aged mice were treated in vitro with a selective Cdc42 activity inhibitor (Sakamori et al., 2012) (newly termed CASIN, referred to in Peterson et al., 2006 as Pirl1-related compound 2) (Y.Z., data not shown, for structure and specificity of CASIN). Treatment with CASIN (5μM) reduced the elevated level of active Cdc42 observed in aged primitive hematopoietic cells to the level observed in young cells (Figures 3A and 3B). CASIN treatment did not alter cell cycle status or apoptosis in aged LT-HSCs (Figures S3A–S3C). In response to treatment with CASIN, LT-HSCs from aged mice showed a dose-dependent increase in the percentage of polarized cells, becoming progressively indistinguishable from young cells (Figures 3C and 3D). These data demonstrate that elevated Cdc42-GTP levels in aged LT-HSCs cell-intrinsically regulate

(C) Percentage of young and aged LT-HSC cells with a polar distribution of Cdc42 and tubulin. Shown are means +1 SE, n = 10; ~500–700 cells scored per sample in total. *p < 0.001.
(D) Percentage of Per-2 polarized cells of Cdc42-polarized young and aged LT-HSCs. Cdc42-polarized cells were analyzed for Per-2 localization and scored positive when Per-2 was found at the Cdc42 pole. Shown are means +1 SE, n = 4, ~150–250 cells scored per sample in total. *p < 0.05.
(E) Representative distribution of Cdc42 and tubulin in young *Cdc42GAP*$^{+/+}$ and *Cdc42GAP*$^{-/-}$ LT-HSCs. Pictures are shown on a dark background (panels i–vi) or as overlap with the phase contrast picture (panels vii and viii). Bar = 5μm.
(F) Percentages of young *Cdc42GAP*$^{+/+}$ (WT Control) and *Cdc42GAP*$^{-/-}$ LT-HSC cells with a polar distribution of Cdc42 and tubulin. Shown are means +1 SE, n = 4, ~200–300 cells scored per sample in total. **p < 0.01, *p < 0.05.
See also Figure S2 and Movies S1–S3.

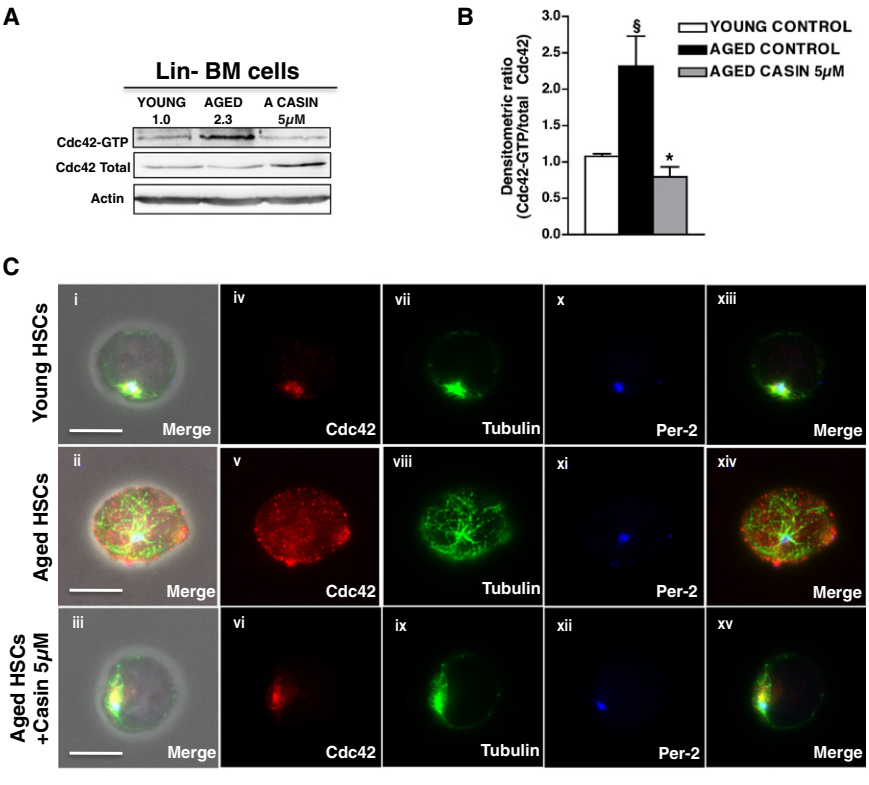

Figure 3. Pharmacological Targeting of Cdc42 Reverts Aged Apolar LT-HSCs to Polar Cells

(A) Representative Cdc42 activity in young, aged, and CASIN (5μM)-treated aged lineage depleted bone marrow (Lin^-BM) as determined by a pull-down/western blot assay. Active Cdc42 (Cdc42-GTP) was normalized with respect to total Cdc42 and actin as delineated by the numbers.

(B) Ratio of the densitometric score of the Cdc42-GTP form and the total Cdc42 expression. Shown are means +1 SE, n = 3, $^{\S}p < 0.05$ versus young control; *p < 0.05 versus aged control.

(C) Representative distribution of Cdc42, tubulin, and Per-2 in young, aged, and aged LT-HSCs treated with 5μM CASIN. Shown are overlaps with the phase contrast picture (panels i–iii) or cells on a dark background (panels iv–xv). Bar = 5 μm.

(D) Percentages of cells polarized for Cdc42 and tubulin in young, aged, and aged LT-HSCs treated with 2.5 and 5μM CASIN. For each sample cells were singularly analyzed and scored for Cdc42 and tubulin polar distribution. Shown are means +1 SE, n = 4, ~200–300 cells scored per sample in total. $^{\S}p < 0.001$ versus young control; ***p < 0.001 versus aged control, **p < 0.01 versus aged control, *p < 0.05 versus aged control.

See also Figure S3.

both Cdc42 and tubulin distribution and that the apolar distribution of these proteins can be reverted to a polar one by decreasing Cdc42 activity. Thus, CASIN treatment reverted aged LT-HSCs to young HSCs with respect to the polarity phenotype.

We next determined whether inhibition of Cdc42 activity in aged LT-HSCs via CASIN treatment could revert at least in part the altered function of aged LT-HSCs to make them become functionally younger. Although CASIN acts transiently on Cdc42 activity, surprisingly, the increase in the percentage of polar cells among aged LT-HSCs induced by CASIN in vitro remained stable for at least up to 6 hr after CASIN withdrawal (Figures S3D and S3E). This result implies a kind of "polarity memory" upon transient reduction of Cdc42 activity in aged LT-HSCs, which might allow continuation of the new polar phenotype and the associated function or functions upon transplantation into recipient animals. Therefore, 200 aged LT-HSCs treated with 5μM CASIN overnight were competitively serially transplanted into young recipients and compared to transplants with young and aged untreated LT-HSCs (Figure 4A). In primary recipients, overall donor engraftment after 8, 16, and 24 weeks was similar in aged control and aged CASIN-treated LT-HSCs (Figure 4B), but remarkably, CASIN treatment of aged LT-HSCs resulted in an increase in contribution to the B cell compartment in PB and a reduced contribution to the myeloid lineage (Figure 4D). In addition, CASIN treatment increased the contribution to LSK and common lymphoid progenitor (CLP) populations to a level indistinguishable from that of young LT-HSCs (Figure S4A). The frequency of donor-derived LT-HSCs among donor-derived LSKs was, as anticipated, doubled in aged control recipients, while upon CASIN treatment this frequency was significantly reduced (Figure 4F). In addition, upon secondary transplant, CASIN-treated LT-HSCs presented with an elevated overall regenerative capacity compared with aged LT-HSCs, as indicated by increased and stable chimerism in PB (Figure 4C). Moreover, upon secondary transplant, CASIN-treated aged LT-HSCs proved to be indistinguishable from young LT-HSCs with respect to B cell and myeloid engraftment in PB and BM (Figure 4E and Figures S4B and S4C) and with respect to the contribution to the LT-HSC pool in BM (Figure 4G). Young CASIN-treated LT-HSCs that were competitively transplanted in experiments alongside the aged control and aged CASIN-treated LT-HSCs transplants did not show any relevant functional changes compared with young control LT-HSCs (Figures S4D–S4K), demonstrating that CASIN reverts specifically aging-related phenotypes of aged LT-HSCs.

Because aged HSCs exhibit a 2-fold reduced ability to home to the BM (Dykstra et al., 2011; Liang et al., 2005) and aged early hematopoietic progenitor cells localize more distantly from the

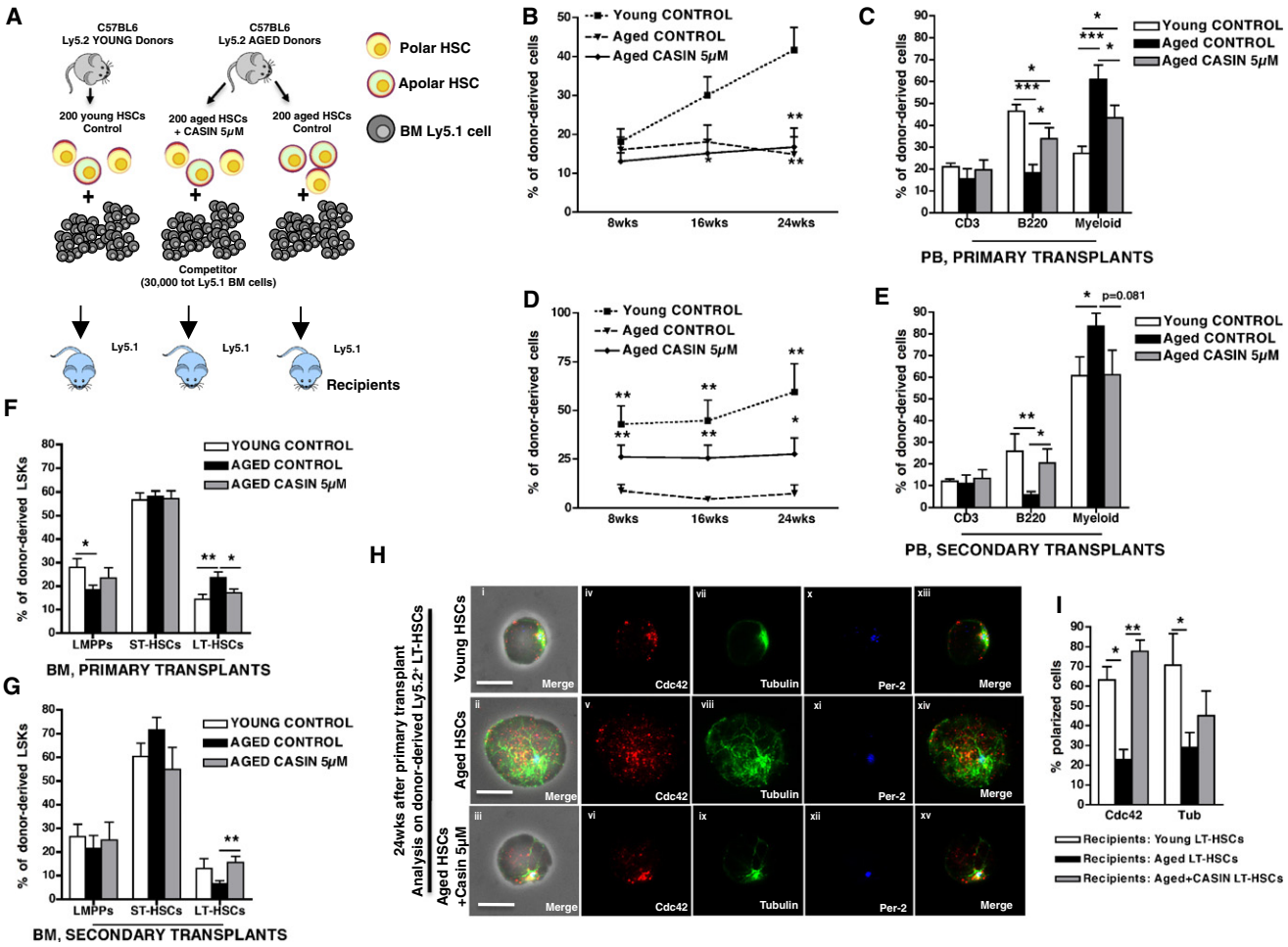

Figure 4. Pharmacological Targeting of Cdc42 Activity Rejuvenates LT-HSC Function

(A) Schematic representation of the experimental setup. Two-hundred aged and young donor ($Ly5.2^+$) LT-HSCs were cultured for 16 hr as indicated and subsequently transplanted into recipient ($Ly5.1^+$) mice along with 3×10^5 BM competitor ($Ly5.1^+$) cells. Twenty-four weeks after transplant, recipient mice were sacrificed and secondary transplants were performed.

(B and D) Percentage of donor contribution ($Ly5.2^+$ cells) to total WBC in PB 8, 16, and 24 weeks after transplant in primary (B) and secondary (D) transplants. Mice were considered as engrafted when the percentage of $Ly5.2^+$ cells in PB was greater than 1.0 in primary transplants and greater than 0.5 in secondary transplants and contribution was detected for all PB lineages. Shown are mean values +1 SE; $^{**}p < 0.01$ and $^{*}p < 0.05$ versus young control in (B); $^{***}p < 0.001$, $^{**}p < 0.01$, $^{*}p < 0.05$ versus aged control in (D).

(C and E) Percentage of $B220^+$, $CD3^+$, and myeloid cells among donor-derived $Ly5.2^+$ cells in PB 24 weeks after primary (C) and secondary (E) transplants. $^{*}p < 0.05$, $^{**}p < 0.01$, $^{***}p < 0.001$; shown are mean values +1 SE.

(F and G) Percentage of LT-HSC, ST-HSC, and LMPP cells in BM among donor-derived LSKs cells 24 weeks after primary (F) and secondary (G) transplants. $^{**}p < 0.01$; shown are mean values +1 SE. Data is based on five (primary transplants) and four (secondary transplants) experimental repeats with five recipient mice per group (e.g., n = 25 for primaries and n = 20 for secondary transplants).

(H) Representative distribution of Cdc42, tubulin, and Per-2 in donor-derived LT-HSCs sorted from young, aged, and aged CASIN-treated LT-HSC recipient mice 24 weeks after transplant. Shown are overlaps with the phase contrast picture (panels i–iii) or cells on a dark background (panels iv–xv). Bar = 5 μm.

(I) Percentage of donor-derived LT-HSCs polarized for Cdc42 and tubulin sorted 24 weeks after transplant from recipient animals competitively reconstituted with young, aged, and aged CASIN-treated LT-HSCs. Shown are mean values +1 SEM, n = 3, ~50 cells scored per sample in total. $^{**}p < 0.01$, $^{*}p < 0.05$.

See also Figure S4.

endosteum compared with the localization of young cells (Kohler et al., 2009), we next investigated whether these aging-associated phenotypes were also rejuvenated by CASIN treatment. Homing of young, aged, and aged CASIN-treated LT-HSCs was determined in competitive short-term homing assays (Dykstra et al., 2011) (Figure S5A), while the distance of LT-HSCs from the endosteum was measured by intravital two-photon microscopy (Kohler et al., 2009). The data indicate that CASIN-treated aged LT-HSC present with significantly improved homing to the BM and localize closer to the endosteum (Figures S5B–S5F) compared with aged control LT-HSCs.

Finally, the frequency of polar donor-derived LT-HSCs in recipients transplanted with aged, aged CASIN-treated, and young primary LT-HSCs was determined 24 weeks after transplantation. The data indicate that the percentage of donor-derived polar LT-HSCs in recipients transplanted with aged

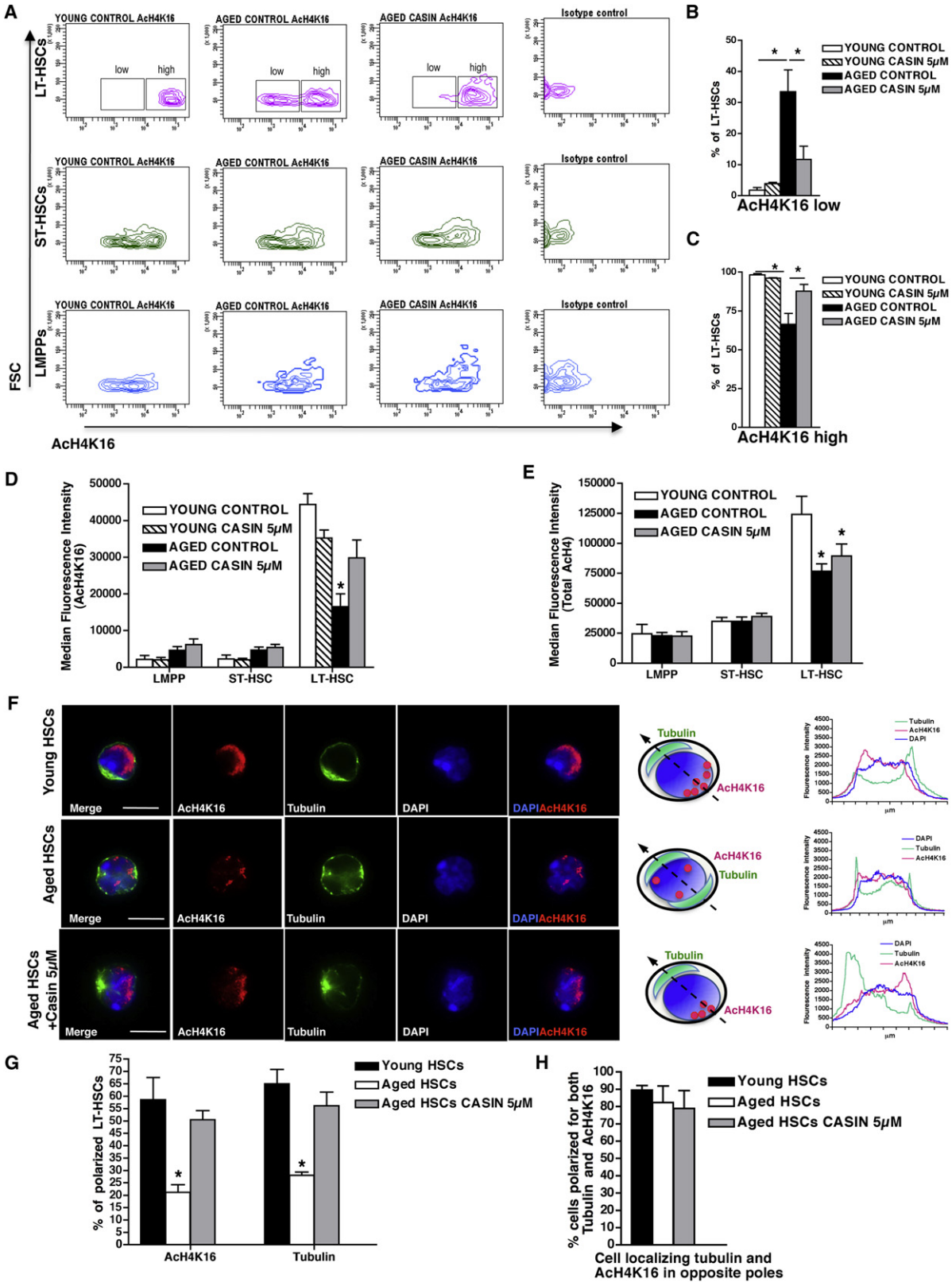

Figure 5. Pharmacological Targeting of Cdc42 Activity Restores the Level and the Spatial Distribution of Histone H4 Lysine 16 Acetylation

(A) Representative FACS density plots of AcH4K16 expression in LT-HSCs, ST-HSCs, and LMPPs. Aged LT-HSCs distribute in two distinct subpopulations expressing low and high AcH4K16 levels.

CASIN-treated LT-HSCs was similar to the frequency found in young controls, and significantly increased, at least with respect to Cdc42 localization, compared with the frequency found in aged untreated controls (Figures 4H and 4I).

One explanation for the long-lasting "memory effect" on aged LT-HSCs upon transient reduction of Cdc42 activity observed in our experiments might be that reduction of Cdc42 activity to the level seen in young LT-HSCs results in epigenetic marker changes in aged LT-HSCs, accordingly with a proposed role for epigenetic regulation of stem cell aging (Pollina and Brunet, 2011; Rando and Chang, 2012). Acetylation of histones is a prevalent epigenetic chromatin modification in eukaryotes. Activated Cdc42 was reported to specifically alter acetylation of histone H4 in 3T3 cells (Alberts et al., 1998), and histone H4 acetylation has been shown to be mitotically stable and inheritable during development (Cavalli and Paro, 1999). On histone H4, lysine 16 is the most common site of acetylation, and controls chromatin structures as well interactions between nonhistone proteins and chromatin fibers, while it is unique as it is the only lysine residue among N-terminal tails of all histones targeted by the Sir2 (or class III) family of HDACs (Vaquero et al., 2007). Histone H4 lysine 16 acetylation (AcH4K16) has been implicated in regulating yeast replicative aging (Dang et al., 2009), and AcH4K16 levels were found to be reduced in multiple tissues of aged mice (Krishnan et al., 2011).

Consequently, we investigated whether elevated Cdc42 activity might affect histone H4 acetylation levels as well as specifically AcH4K16 patterns in primitive hematopoietic cells including LT-HSCs. Our data demonstrate that young LT-HSCs express higher levels of AcH4K16 than young ST-HSCs and LMPPs do (Figures 5A and 5D), in agreement with previous reports (Chung et al., 2009). Aged LT-HSCs present with an overall decreased level of AcH4K16 compared with young LT-HSCs, but still show higher levels of AcH4K16 compared with aged ST-HSCs and LMPPs (Figures 5A and 5D). Moreover, aged LT-HSCs only present with two distinct subpopulations expressing low and high AcH4K16 levels (Figure 5A), which are not found in young LT-HSCs. Young LT-HSCs are almost exclusively AcH4K16^{high} cells while 34% of aged LT-HSCs present with a low AcH4K16 expression level. CASIN treatment induces a sharp decrease of the frequency of AcH4K16^{low} aged LT-HSCs while increasing the frequency of AcH4K16^{high} cells (Figures 5A–5C). This effect of CASIN on AcH4K16 (Figures 5A–5D) was specific to LT-HSCs (no effect on ST-HSCs and LMPPs), age specific (young CASIN-treated LT-HSCs did not display any significant modification), and specific to acetylation of lysine 16 on histone H4 (the total level of acetylation on histone H4 was not altered; Figure 5E). Most interestingly, we observed that AcH4K16 localization within the nucleus of young LT-HSCs was polarized and opposite that of the cytoplasmatic tubulin pole, while the great majority of aged LT-HSCs nuclei were apolar for AcH4K16 localization (Figures 5F–5H and Movies S4 and S5). Strikingly, CASIN treatment of aged LT-HSCs increased the frequency of aged LT-HSCs with a polar localization of AcH4K16 to a level similar to that found in young LT-HSCs (Figures 5F–5H). Thus treatment of aged LT-HSCs with CASIN restores the level and the spatial distribution of AcH4K16 to the level seen in young LT-HSCs, consistent with a previous suggested loss of epigenetic regulation in aged HSCs (Chambers et al., 2007; Pollina and Brunet, 2011). Importantly, our data does not exclude the possibility that inhibition of Cdc42 activity in aged LT-HSCs might also alter additional epigenetic marks like histone methylation patterns.

In summary, these data identify elevated Cdc42 activity as a key modulator of a molecular pathway driving intrinsic mechanisms of stem cell aging. Furthermore, these results demonstrate that lowering Cdc42 activity by CASIN treatment rejuvenates aged LT-HSCs with respect to function (lineage skewing, regenerative capacity, and homing) and phenotypic (polarity) and epigenetic (AcH4K16, both level of acetylation and localization within the nucleus) parameters.

DISCUSSION

Until recently, there was a broad consensus that the phenotype of aged HSCs is fixed and dominated by cell-intrinsic regulatory mechanisms that could not be reverted by therapeutic intervention. This paradigm recently started to shift (Rando and Chang, 2012), because it was demonstrated that impaired contribution to PB upon transplantation of aged HSCs could be ameliorated by either antioxidative therapy or rapamycin treatment (Chen et al., 2009; Ito et al., 2006). Our data significantly extend these observations as we demonstrate a critical mechanistic role of Cdc42 activity in HSC aging and identify it as a target for pharmacological rejuvenation of stem-cell-intrinsic age-associated phenotypes of LT-HSCs. Also, because the differences in polarity between young and aged LT-HSCs with respect to Cdc42, tubulin, and AcH4K16 are regulated by Cdc42 activity, these data further support a novel concept in which aging-associated changes in LT-HSC self-renewal and differentiation are possibly regulated by changes in stem cell polarity. Our data further identify a role for Cdc42 activity in regulating epigenetic modifications in LT-HSCs and polarity of epigenetic markers (epi-polarity), and identify the loss of this polarity upon aging as a key concept in HSC biology. Interestingly, a recent

(B and C) Percentage of LT-HSCs expressing low (B) and high (C) levels of AcH4K16 according to the gating shown in (A).
(D and E) Median fluorescence intensity detected for AcH4K16 (D) and total AcH4 (E) in LT-HSCs, ST-HSCs, and LMPPs. Shown are mean values +1 SEM, n = 3. *$p < 0.05$.
(F) Representative distribution of AcH4K16 (red) and tubulin (green) in young, aged, and aged LT-HSCs treated with 5μM CASIN. Nuclei are stained with DAPI (blue). Bar = 5 μm. Schemes of tubulin and AcH4K16 distributions in young, aged, and aged LT-HSCs treated with 5μM CASIN and relative fluorescence intensity plot obtained by collecting pixel intensity through the section of the relative cell are also shown.
(G) Percentages of cells polarized for AcH4K16 and tubulin in young, aged, and aged CASIN-treated (5μM) LT-HSCs. For each sample cells were singularly analyzed and scored for AcH4K16 and tubulin polar distribution. The percentage of polarized cells is plotted over the total number of cells scored.
(H) Percentages of cells polarized for AcH4K16 and tubulin in opposite poles in young, aged, and aged CASIN-treated (5μM) LT-HSCs. The percentage of cells showing opposite polarity is plotted over the number of cells polarized for both markers. Shown are means +1 SE, n = 3, ~100–150 cells scored per sample in total. *$p < 0.01$.
See also Figure S5 and Movies S4 and S5.

report described a prominent role for epigenetic modifications in transgenerational and thus long-term-memory-associated longevity in *C. elegans* (Greer et al., 2011). Furthermore, genome-wide association studies have recently identified a positive correlation between *Cdc42* expression in human white blood cells and increased morbidity and aging (Kerber et al., 2009), while elevated Cdc42 activity was found in multiple tissues of aged mice, likely implying a role for the Cdc42-polarity pathway in aging not only of LT-HSCs.

EXPERIMENTAL PROCEDURES

Serial Competitive Transplantation

BM cells (10^6) from 4- to 6-week-old *Cdc42GAP*$^{+/+}$ and *Cdc42GAP*$^{-/-}$ mice and aged (20- to 26-month-old) C57BL/6 mice (donors, Ly5.2$^+$) were mixed with 10^6 BM cells from young (2- to 4-month-old) BoyJ competitor mice (Ly5.1$^+$) and injected into the retro-orbital sinus of irradiated BoyJ recipient mice (Ly5.1$^+$) in 200 μl in PBS. Primary transplanted mice were sacrificed after 20 weeks and 2 × 10^6 BM cells from each recipient mouse were injected into a secondary preconditioned recipient BoyJ mouse. Serial BM transplantation experiments were repeated three times with a cohort of four or five recipient mice per donor. For competitive LT-HSC transplantation, young (2- to 4-month-old) and aged (20- to 26-month-old) C57BL/6 mice (Ly5.2$^+$) were used as donors. Two-hundred LT-HSCs were sorted into 96 multiwell plates and cultured (either in suspension or adherent to fibronectin) for 16 hr in HBSS + 10% FBS ± CASIN (5μM) in a water-jacketed incubator at 37°C (5% CO_2, 3% O_2). Stem cells were then mixed with 3 × 10^5 BM cells from young (2- to 4-month-old) BoyJ competitor mice (Ly5.1$^+$) and then transplanted into BoyJ recipient mice (Ly5.1$^+$). PB chimerism was determined by FACS analysis every 8 weeks. Twenty-four weeks after primary transplants, 2 × 10^6 BM cells from an individual primary recipient mouse were injected into an individual secondary preconditioned recipient BoyJ mouse. Experiments were performed three times with LT-HSCs cultured in suspension and two times with LT-HSCs cultured on a fibronectin-coated substrate without any difference in experimental outcome. Primary transplanted mice were regarded engrafted when PB chimerism was greater or equal to 1.0% and contribution was detected in all lineages. Secondary transplanted mice were regarded as engrafted when PB chimerism was greater or equal to 0.5% and contribution was detected in all lineages.

Flow Cytometry and Cell Sorting

PB and BM cell immunostaining was performed according to standard procedures, and samples were analyzed on an LSRII flow cytometer (BD Biosciences). Lineage FACS analysis data are plotted as the percentages of B220$^+$, CD3$^+$, and Myeloid (Gr-1$^+$, Mac-1$^+$, and Gr-1$^+$Mac-1$^+$) cells among donor-derived Ly5.2$^+$ cells. As for early hematopoiesis analysis, mononuclear cells were isolated by low-density centrifugation (Histopaque 1083, Sigma) and stained with a cocktail of biotinylated lineage antibodies. After lineage depletion by magnetic separation (Dynalbeads, Invitrogen), cells were stained with anti-Sca-1 (clone D7) (eBioscience), anti-c-Kit (clone 2B8) (eBioscience), anti-CD34 (clone RAM34) (eBioscience), anti-CD127 (clone A7R34) (eBioscience), anti-Flk2 (clone A2F10) (eBioscience), and Streptavidin (eBioscience). Early hematopoiesis FACS analysis data were plotted as the percentage of LT-HSC (gated as LSK CD34$^{-/low}$Flk2$^-$), ST-HSC (gated as LSK CD34$^+$Flk2$^-$), and LMPP (gated as LSK CD34$^+$Flk2$^+$) (Adolfsson et al., 2005) distribution among donor-derived LSKs (Lin$^-$c-Kit$^+$Sca-1$^+$ cells). LSK and CLPs (gated as Lin$^-$c-Kit$^{+/low}$Sca-1$^{+/low}$IL7Rα$^+$) (Karsunky et al., 2008) were plotted as percentages among donor-derived Lin$^-$ cells. In order to isolate LT-HSCs, lineage depletion was performed to enrich for lineage-negative cells. Lineage-negative cells were then stained as aforementioned and sorted using a BD FACS Aria I or a BD FACS Aria III (BD Bioscience). For intracellular flow cytometric staining of AcH4 and AcH4K16, lineage-depleted young and aged BM cells were incubated for 16 hr with or without CASIN (5μM) in IMDM + 10% FBS at 37°C (5%CO_2, 3%O_2). At the end of the treatment, the samples were moved on ice and stained again with the cocktail of biotinylated lineage antibodies. After being washed the samples were stained with anti-Sca-1 (clone D7) (eBioscience), anti-c-Kit (clone 2B8) (eBioscience), anti-CD34 (clone RAM34) (eBioscience), anti-Flk2 (clone A2F10) (eBioscience), and Streptavidin (eBioscience). At the end of the surface staining, cells were fixed and permeabilized with Cytofix/Cytoperm Solution (BD Biosciences) and incubated with 10% Donkey Serum (Sigma) in BD Perm/Wash Buffer (BD Biosciences) for 30 min. Primary and secondary antibody incubations were performed at room temperature in BD Perm/Wash Buffer (BD Biosciences) for 1 hr and 30 min, respectively. The primary antibodies for AcH4 were obtained all by Upstate-Millipore (rabbit anti-acetyl-histone H4 Lys5, Lys8, Lys12, and Lys16). The secondary antibody is a donkey anti-rabbit DyLight649 (BioLegend).

IF Staining

Freshly sorted LT-HSCs were seeded on fibronectin-coated glass coverslips in HBSS + 10% FBS. CASIN (referred to in Peterson et al., 2006 as Pirl1-related compound 2) was obtained from Chembridge Corporation, and purified to greater than 99% by high-performance liquid chromatography. After 16 hr of incubation at 37°C (5% CO_2, 3% O_2) in growth factors-free medium, cells were fixed with BD Cytofix Fixation Buffer (BD Biosciences). After fixation cells were gently washed with PBS, permeabilized with 0.2% Triton X-100 (Sigma) in PBS for 20 min, and blocked with 10% Donkey Serum (Sigma) for 30 min. Primary and secondary antibody incubations were performed for 1 hr at room temperature. Coverslips were mounted with ProLong Gold Antifade Reagent with or without DAPI (Invitrogen, Molecular Probes). The cells were coimmunostained with an anti-alpha tubulin antibody (Abcam, rat monoclonal ab6160) detected with an anti-rat AMCA-conjugated secondary antibody or an anti-rat DyLight488-conjugated antibody (Jackson ImmunoResearch), an anti-Cdc42 antibody (Millipore, rabbit polyclonal) or an anti-AcH4K16 antibody (Upstate-Millipore, rabbit polyclonal) detected with an anti-rabbit DyLight549-conjugated antibody (Jackson ImmunoResearch), and/or an anti-Pericentrin-2 antibody (Santa Cruz Biotechnology, goat polyclonal) detected with an anti-goat AMCA-conjugated antibody (Jackson ImmunoResearch). Samples were imaged with an AxioObserver Z1 microscope (Zeiss) equipped with a 63× PH objective. Images were analyzed with AxioVision 4.6 software. Alternatively, samples were analyzed with an LSM710 confocal microscope (Zeiss) equipped with a 63× objective. Primary raw data were imported into the Volocity Software package (Version 6.0, Perkin Elmer) for further processing and conversion into 3D images. As for polarity scoring, the localization of each single-stained protein was considered polarized when a clear asymmetric distribution was visible by drawing a line across the middle of the cell. A total of 50 to 100 LT-HSCs were singularly analyzed per sample. Data are plotted as percentage of the total number of cells scored per sample. Specificity of the anti-Cdc42 antibody in IF was tested on LT-HSCs sorted from mice in which *Cdc42* was targeted and deleted specifically in the hematopoietic system (Mx1-Cre;Cdc42$^{flox/flox}$ mice; Yang et al., 2007) (data not shown).

Competitive Short-Term Homing Assay and Intravital Two-Photon Microscopy

For competitive short-term homing assay (Dykstra et al., 2011), LT-HSCs were sorted from young and aged mice and incubated for 16 hr in HBSS + 10% FBS ± CASIN (5μM) in a water-jacketed incubator at 37°C (5% CO_2, 3% O_2). After treatment, LT-HSCs were labeled with the cell tracker CFSE (Invitrogen-Molecular probes) or the cell tracker CMRA (Invitrogen-Molecular probes), washed, and mixed, so that 5,000 young + 5,000 aged LT-HSCs or 5,000 aged + 5,000 aged CASIN-treated LT-HSCs could be injected into each lethally irradiated young recipient mouse (figure S4L). After 16–18 hr from the stem cell injection, recipient mice were sacrificed and all BM cells were analyzed by flow cytometry so we could quantify relative frequency of CFSE$^+$ and CMRA$^+$ cells. A total of six recipient mice were injected per experiment (three receiving 5,000 CFSE$^+$ young LT-HSCs mixed with 5,000 CMRA$^+$ aged LT-HSCs each, and three receiving 5,000 CFSE$^+$ aged CASIN-treated LT-HSCs mixed with 5,000 CMRA$^+$ aged LT-HSCs each), and the experiment was repeated twice. For intravital two-photon microscopy analysis, LT-HSCs were sorted, treated, labeled, and mixed as aforementioned but injected into nonirradiated recipient young mice. A total of four recipient mice were injected per experiment (two receiving 5,000 CFSE$^+$ young LT-HSCs mixed with 5,000 CMRA$^+$ aged LT-HSCs each, and two receiving 5,000 CFSE$^+$ aged

CASIN-treated LT-HSCs mixed with 5,000 CMRA$^+$ aged LT-HSCs each). After 16–18 hr from the stem cell injection, recipient mice were prepared for intravital microscopy as previously described (Kohler et al., 2009) using isofluran-based intubation narcosis. Briefly, the tibiae were exposed and part of the bone tissue was carefully removed with an electric drill (Dremel) to obtain a very thin (30–50 μm) remaining layer of bone tissue covering the BM cavity. This procedure was permanently controlled by stereomicroscopy. The bone tissue was identified due to its strong autofluorescence (CCD) under unaltered light conditions or using its second-harmonic (SHG) signal (PMT). Animals were kept at 37°C in a PBS water bath while experiments were performed. For imaging, the area was scanned down to ~120 μm depth (more than 12 cell layers) using an illumination wavelength of either 800 or 880 nm detecting CFSE (530 nm) and CMRA (580 nm) fluorescence, as well as unaltered light or SHG (at 480 nm emission). Primary raw data were imported into the Volocity Software package (Version 6.0, Perkin Elmer) for further processing and conversion into 3D images and for measurement of the distance between LT-HSCs and the endosteum.

SUPPLEMENTAL INFORMATION

Supplemental Information for this article includes five figures, five movies, and Supplemental Experimental Procedures and can be found with this article online at doi:10.1016/j.stem.2012.04.007.

ACKNOWLEDGMENTS

We thank Gary Van Zant, Jose A. Cancelas, Marnie A. Ryan, and Hartmut Weiler for advice and critical reading of the manuscript. We thank Frank Kirchhoff and Dré van der Merwe for cell sorting support, Angelika Rück and the Institut für Lasertechnologien in der Medizin und Meßtechnik of Ulm University for support with confocal microscopy, and the Tierforschungszentrum of the University of Ulm for supporting our animal work. This work was supported by grants from the Deutsche Forschungsgemeinschaft (KFO 142, GE2063/1) and from the National Institute of Health (HL076604, DK077762, and AG040118) to H.G., and by a "Bausteinprogramm" of the Department of Medicine Ulm to M.C.F. M.C.F. and H.G. designed and interpreted experiments and wrote the manuscript. M.C.F. performed and analyzed experiments. H.G. helped in performing transplantation experiments. K.D. and D.D. assisted in transplantation procedures and K.D, D.D., M.R., and H.S aided with cell sorting and flow analysis procedures. A.N. assisted in transplantation procedures and supported the Cdc42GAP mouse colony. A.H. and M.G. supported experiments with respect to intra-vital imaging. M.-D.F., K.S-K., and Y.Z. assisted in designing and interpreting experiments. The authors declare no competing financial interests.

Received: August 30, 2011
Revised: February 29, 2012
Accepted: April 9, 2012
Published: May 3, 2012

REFERENCES

Adolfsson, J., Månsson, R., Buza-Vidas, N., Hultquist, A., Liuba, K., Jensen, C.T., Bryder, D., Yang, L., Borge, O.J., Thoren, L.A., et al. (2005). Identification of Flt3+ lympho-myeloid stem cells lacking erythro-megakaryocytic potential a revised road map for adult blood lineage commitment. Cell *121*, 295–306.

Alberts, A.S., Geneste, O., and Treisman, R. (1998). Activation of SRF-regulated chromosomal templates by Rho-family GTPases requires a signal that also induces H4 hyperacetylation. Cell *92*, 475–487.

Barfod, E.T., Zheng, Y., Kuang, W.J., Hart, M.J., Evans, T., Cerione, R.A., and Ashkenazi, A. (1993). Cloning and expression of a human CDC42 GTPase-activating protein reveals a functional SH3-binding domain. J. Biol. Chem. *268*, 26059–26062.

Beerman, I., Bhattacharya, D., Zandi, S., Sigvardsson, M., Weissman, I.L., Bryder, D., and Rossi, D.J. (2010). Functionally distinct hematopoietic stem cells modulate hematopoietic lineage potential during aging by a mechanism of clonal expansion. Proc. Natl. Acad. Sci. USA *107*, 5465–5470.

Beghé, C., Wilson, A., and Ershler, W.B. (2004). Prevalence and outcomes of anemia in geriatrics: a systematic review of the literature. Am. J. Med. *116* (*Suppl 7A*), 3S–10S.

Cappello, S., Attardo, A., Wu, X., Iwasato, T., Itohara, S., Wilsch-Bräuninger, M., Eilken, H.M., Rieger, M.A., Schroeder, T.T., Huttner, W.B., et al. (2006). The Rho-GTPase cdc42 regulates neural progenitor fate at the apical surface. Nat. Neurosci. *9*, 1099–1107.

Cau, J., and Hall, A. (2005). Cdc42 controls the polarity of the actin and microtubule cytoskeletons through two distinct signal transduction pathways. J. Cell Sci. *118*, 2579–2587.

Cavalli, G., and Paro, R. (1999). Epigenetic inheritance of active chromatin after removal of the main transactivator. Science *286*, 955–958.

Chambers, S.M., and Goodell, M.A. (2007). Hematopoietic stem cell aging: wrinkles in stem cell potential. Stem Cell Rev. *3*, 201–211.

Chambers, S.M., Shaw, C.A., Gatza, C., Fisk, C.J., Donehower, L.A., and Goodell, M.A. (2007). Aging hematopoietic stem cells decline in function and exhibit epigenetic dysregulation. PLoS Biol. *5*, e201.

Chang, J.T., Palanivel, V.R., Kinjyo, I., Schambach, F., Intlekofer, A.M., Banerjee, A., Longworth, S.A., Vinup, K.E., Mrass, P., Oliaro, J., et al. (2007). Asymmetric T lymphocyte division in the initiation of adaptive immune responses. Science *315*, 1687–1691.

Chen, C., Liu, Y., Liu, Y., and Zheng, P. (2009). mTOR regulation and therapeutic rejuvenation of aging hematopoietic stem cells. Sci. Signal. *2*, ra75.

Cheng, J., Türkel, N., Hemati, N., Fuller, M.T., Hunt, A.J., and Yamashita, Y.M. (2008). Centrosome misorientation reduces stem cell division during ageing. Nature *456*, 599–604.

Chung, Y.S., Kim, H.J., Kim, T.M., Hong, S.H., Kwon, K.R., An, S., Park, J.H., Lee, S., and Oh, I.H. (2009). Undifferentiated hematopoietic cells are characterized by a genome-wide undermethylation dip around the transcription start site and a hierarchical epigenetic plasticity. Blood *114*, 4968–4978.

Dang, W., Steffen, K.K., Perry, R., Dorsey, J.A., Johnson, F.B., Shilatifard, A., Kaeberlein, M., Kennedy, B.K., and Berger, S.L. (2009). Histone H4 lysine 16 acetylation regulates cellular lifespan. Nature *459*, 802–807.

Dorshkind, K., and Swain, S. (2009). Age-associated declines in immune system development and function: causes, consequences, and reversal. Curr. Opin. Immunol. *21*, 404–407.

Dykstra, B., Olthof, S., Schreuder, J., Ritsema, M., and de Haan, G. (2011). Clonal analysis reveals multiple functional defects of aged murine hematopoietic stem cells. J. Exp. Med. *208*, 2691–2703.

Ergen, A.V., and Goodell, M.A. (2009). Mechanisms of hematopoietic stem cell aging. Exp. Gerontol. *45*, 286–290.

Etienne-Manneville, S. (2004). Cdc42—the centre of polarity. J. Cell Sci. *117*, 1291–1300.

Florian, M.C., and Geiger, H. (2010). Concise review: polarity in stem cells, disease, and aging. Stem Cells *28*, 1623–1629.

Geiger, H., and Rudolph, K.L. (2009). Aging in the lympho-hematopoietic stem cell compartment. Trends Immunol. *30*, 360–365.

Geiger, H., and Van Zant, G. (2002). The aging of lympho-hematopoietic stem cells. Nat. Immunol. *3*, 329–333.

Geiger, H., Rennebeck, G., and Van Zant, G. (2005). Regulation of hematopoietic stem cell aging in vivo by a distinct genetic element. Proc. Natl. Acad. Sci. USA *102*, 5102–5107.

Geiger, H., Koehler, A., and Gunzer, M. (2007). Stem cells, aging, niche, adhesion and Cdc42: a model for changes in cell-cell interactions and hematopoietic stem cell aging. Cell Cycle *6*, 884–887.

Greer, E.L., Maures, T.J., Ucar, D., Hauswirth, A.G., Mancini, E., Lim, J.P., Benayoun, B.A., Shi, Y., and Brunet, A. (2011). Transgenerational epigenetic inheritance of longevity in Caenorhabditis elegans. Nature *479*, 365–371.

Iden, S., and Collard, J.G. (2008). Crosstalk between small GTPases and polarity proteins in cell polarization. Nat. Rev. Mol. Cell Biol. *9*, 846–859.

Ito, K., Hirao, A., Arai, F., Takubo, K., Matsuoka, S., Miyamoto, K., Ohmura, M., Naka, K., Hosokawa, K., Ikeda, Y., and Suda, T. (2006). Reactive oxygen species act through p38 MAPK to limit the lifespan of hematopoietic stem cells. Nat. Med. *12*, 446–451.

Janzen, V., Forkert, R., Fleming, H.E., Saito, Y., Waring, M.T., Dombkowski, D.M., Cheng, T., DePinho, R.A., Sharpless, N.E., and Scadden, D.T. (2006). Stem-cell ageing modified by the cyclin-dependent kinase inhibitor p16INK4a. Nature *443*, 421–426.

Ju, Z., Jiang, H., Jaworski, M., Rathinam, C., Gompf, A., Klein, C., Trumpp, A., and Rudolph, K.L. (2007). Telomere dysfunction induces environmental alterations limiting hematopoietic stem cell function and engraftment. Nat. Med. *13*, 742–747.

Kamminga, L.M., van Os, R., Ausema, A., Noach, E.J., Weersing, E., Dontje, B., Vellenga, E., and de Haan, G. (2005). Impaired hematopoietic stem cell functioning after serial transplantation and during normal aging. Stem Cells *23*, 82–92.

Karsunky, H., Inlay, M.A., Serwold, T., Bhattacharya, D., and Weissman, I.L. (2008). Flk2+ common lymphoid progenitors possess equivalent differentiation potential for the B and T lineages. Blood *111*, 5562–5570.

Kerber, R.A., O'Brien, E., and Cawthon, R.M. (2009). Gene expression profiles associated with aging and mortality in humans. Aging Cell *8*, 239–250.

Kiss, T.L., Sabry, W., Lazarus, H.M., and Lipton, J.H. (2007). Blood and marrow transplantation in elderly acute myeloid leukaemia patients - older certainly is not better. Bone Marrow Transplant. *40*, 405–416.

Kohler, A., Schmithorst, V., Filippi, M.D., Ryan, M.A., Daria, D., Gunzer, M., and Geiger, H. (2009). Altered cellular dynamics and endosteal location of aged early hematopoietic progenitor cells revealed by time-lapse intravital imaging in long bones. Blood *114*, 290–298.

Krishnan, V., Chow, M.Z., Wang, Z., Zhang, L., Liu, B., Liu, X., and Zhou, Z. (2011). Histone H4 lysine 16 hypoacetylation is associated with defective DNA repair and premature senescence in Zmpste24-deficient mice. Proc. Natl. Acad. Sci. USA *108*, 12325–12330.

Liang, Y., Van Zant, G., and Szilvassy, S.J. (2005). Effects of aging on the homing and engraftment of murine hematopoietic stem and progenitor cells. Blood *106*, 1479–1487.

Linton, P.J., and Dorshkind, K. (2004). Age-related changes in lymphocyte development and function. Nat. Immunol. *5*, 133–139.

Ludford-Menting, M.J., Oliaro, J., Sacirbegovic, F., Cheah, E.T., Pedersen, N., Thomas, S.J., Pasam, A., Iazzolino, R., Dow, L.E., Waterhouse, N.J., et al. (2005). A network of PDZ-containing proteins regulates T cell polarity and morphology during migration and immunological synapse formation. Immunity *22*, 737–748.

Morrison, S.J., Wandycz, A.M., Akashi, K., Globerson, A., and Weissman, I.L. (1996). The aging of hematopoietic stem cells. Nat. Med. *2*, 1011–1016.

Peterson, J.R., Lebensohn, A.M., Pelish, H.E., and Kirschner, M.W. (2006). Biochemical suppression of small-molecule inhibitors: a strategy to identify inhibitor targets and signaling pathway components. Chem. Biol. *13*, 443–452.

Pollina, E.A., and Brunet, A. (2011). Epigenetic regulation of aging stem cells. Oncogene *30*, 3105–3126.

Rando, T.A. (2006). Stem cells, ageing and the quest for immortality. Nature *441*, 1080–1086.

Rando, T.A., and Chang, H.Y. (2012). Aging, rejuvenation, and epigenetic reprogramming: resetting the aging clock. Cell *148*, 46–57.

Rossi, D.J., Bryder, D., Zahn, J.M., Ahlenius, H., Sonu, R., Wagers, A.J., and Weissman, I.L. (2005). Cell intrinsic alterations underlie hematopoietic stem cell aging. Proc. Natl. Acad. Sci. USA *102*, 9194–9199.

Rossi, D.J., Seita, J., Czechowicz, A., Bhattacharya, D., Bryder, D., and Weissman, I.L. (2007). Hematopoietic stem cell quiescence attenuates DNA damage response and permits DNA damage accumulation during aging. Cell Cycle *6*, 2371–2376.

Rossi, D.J., Jamieson, C.H., and Weissman, I.L. (2008). Stems cells and the pathways to aging and cancer. Cell *132*, 681–696.

Sakamori, R., Das, S., Yu, S., Feng, S., Stypulkowski, E., Guan, Y., Douard, V., Tang, W., Ferraris, R.P., Harada, A., et al. (2012). Cdc42 and Rab8a are critical for intestinal stem cell division, survival, and differentiation in mice. J. Clin. Invest. *122*, 1052–1065.

Sengupta, A., Duran, A., Ishikawa, E., Florian, M.C., Dunn, S., Fickera, A., Leitgese, M., Geiger, H., Diaz-Mecob, M., Moscatb, J., et al. (2011). Atypical protein kinase C (aPKCζ and aPKCλ) is dispensable for mammalian hematopoietic stem cell activity and blood formation. Proc. Natl. Acad. Sci. U S A *108*, 9957–9962.

Signer, R.A., Montecino-Rodriguez, E., Witte, O.N., McLaughlin, J., and Dorshkind, K. (2007). Age-related defects in B lymphopoiesis underlie the myeloid dominance of adult leukemia. Blood *110*, 1831–1839.

Silva, H., and Conboy, I.M. (2008). Aging and stem cell renewal. StemBook, The Stem Cell Research Community (Cambridge, MA: Harvard Stem Cell Institute).

Sinha, S., and Yang, W. (2008). Cellular signaling for activation of Rho GTPase Cdc42. Cell. Signal. *20*, 1927–1934.

Sudo, K., Ema, H., Morita, Y., and Nakauchi, H. (2000). Age-associated characteristics of murine hematopoietic stem cells. J. Exp. Med. *192*, 1273–1280.

Vaquero, A., Sternglanz, R., and Reinberg, D. (2007). NAD+-dependent deacetylation of H4 lysine 16 by class III HDACs. Oncogene *26*, 5505–5520.

Wang, L., Yang, L., Debidda, M., Witte, D., and Zheng, Y. (2007). Cdc42 GTPase-activating protein deficiency promotes genomic instability and premature aging-like phenotypes. Proc. Natl. Acad. Sci. USA *104*, 1248–1253.

Xing, Z., Ryan, M.A., Daria, D., Nattamai, K.J., Van Zant, G., Wang, L., Zheng, Y., and Geiger, H. (2006). Increased hematopoietic stem cell mobilization in aged mice. Blood *108*, 2190–2197.

Yang, L., Wang, L., Kalfa, T.A., Cancelas, J.A., Shang, X., Pushkaran, S., Mo, J., Williams, D.A., and Zheng, Y. (2007). Cdc42 critically regulates the balance between myelopoiesis and erythropoiesis. Blood *110*, 3853–3861.